UMHEP-398
September 1993

The reactions $\gamma\gamma \to W_L^+ W_L^-$ and $\gamma\gamma \to Z_L Z_L$ in $SU(N)$ strongly interacting theories

John F. Donoghue* **and Tibor Torma†**

Department of Physics
University of Massachusetts
Amherst, MA 01003 U.S.A.

Abstract

Building on recent phenomenology of $\gamma\gamma \to \pi\pi$, we discuss the expectation for two photon production of longitudinal gauge boson pairs in $SU(N)$ technicolor theories. The treatment involves a matching of dispersive techniques with the methodology of chiral perturbation theory.

*e–mail: donoghue@phast.umass.edu
†e–mail: kakukk@phast.umass.edu

I. Introduction

If the symmetry breaking part of the Standard Model is strongly interacting, it becomes important to study reactions involving longitudinal gauge bosons. These reactions may yield information on the underlying mechanism of symmetry breaking. The case of $W_L^+W_L^- \to W_L^+W_L^-$ scattering has been extensively explored [1]. Photon production of longitudinal bosons, $\gamma\gamma \to W_LW_L$, may also be an interesting reaction to study, and it has been discussed increasingly recently [2],[3]. Because the equivalence theorem [20][21][22][23] relates the longitudinal gauge boson coupling to those of the original scalars /pseudoscalars of the underlying theory when the energy is high enough, the discussion may also be phrased in terms of the production of the Goldstone bosons. The corresponding reactions in QCD, $\gamma\gamma \to \pi\pi$, has recently had extensive theoretical investigations as well as comparison with experiment, and the connection between the chiral constraints and dispersion theory have been resolved. Since we appear to have now a theoretical control over this reaction, it is of interest to display the expectations for an $SU(N)$ QCD-like theory, scaled up to TeV energies. If the symmetry breaking sector is due to fermion condensates, such as may occur in technicolor, these expectations could possibly be realized by Nature. If not, these results may still form a useful contrast with other possibilities, such as a strongly interacting Higgs theory. In this paper we apply the formulation of Ref. [4] to the reactions $\gamma\gamma \to WW$.

There have been two recent papers [2],[3] which show several similarities with our work, with the most extensive exploration of the phenomenological consequences being given by Herrero and Ruiz-Morales [3]. Our paper is different in its dispersive treatment and in its use of recent experimental and theoretical work on the $\gamma\gamma \to \pi\pi$ reaction. We also emphasize the importance of techni-f_2-like resonances in the direct channel.

The paper proceeds as follows. In Sect. II., we review the essential features of the QCD reaction $\gamma\gamma \to \pi\pi$, and explain in general how this may be transformed to an $SU(N)$ theory at TeV scales. Sect. III. describes the details of the calculation, and presents the results. In an appendix we discuss the use of the equivalence theorem in loop diagrams.

[0]This work has been supported in part by the National Science Foundation

II. $\gamma\gamma \to \pi\pi$ and a model for $\gamma\gamma \to WW, ZZ$

The two important tools in the analysis of $\gamma\gamma \to \pi\pi$ are chiral symmetry and dispersion relations. Early work describing the one loop chiral calculation of $\gamma\gamma \to \pi^0\pi^0$ yielded results which, while valid for small enough pion mass, receive significant corrections even at the physical threshold. These corrections have been seen in a two loop chiral calculation [5] and in dispersive studies [4],[11], and are also needed experimentally. Since the chiral results for this particular reaction are modified at such a low energy, one needs to use other methods in order to work at higher energies. Dispersion relations are useful in this regard. In fact, the two techniques work well together, since chiral symmetry allows one to identify the substraction constants which appear in dispersive treatments.

However, because dispersion relations are a methodology, not an underlying theory, the result are only as good as the inputs to the calculations. While theorists have become reasonably adept at identifying the appropriate input, it is valuable to have experimental data to verify the results.

The starting point is a dispersive representation for the $\gamma\gamma \to \pi\pi$ S-wave amplitude with isospin I,

$$f_I(s) = t_I(s) + D_I^{-1}(s)\{(c_I + d_I s) - \frac{s^2}{\pi}\int_{4m_\pi^2}^{\infty} \frac{dx}{x^2}\frac{t_I(x) Im D_I(x)}{x - s - i\epsilon}\} \qquad (1)$$

originally given by Morgan and Pennington [9]. Here, $t_I(s)$ is a real function which contains all of the correct cuts of the t-channel process $\gamma\pi \to \gamma\pi$, $D_I^{-1}(s)$ is the Omnès function which can be obtained from $\pi\pi$ scattering, and c_I, d_I are substraction constants. The dispersion relation is valid below inelastic thresholds. In order to have a succesful calculation, one must specify correctly the three ingredients listed above. In Ref. [4], this was accomplished as follows. By comparison with the one loop calculation in chiral perturbation theory, the substraction constants are identified as

$$c_0 = c_2 = 0 \qquad (2)$$

$$d_0 = d_2 = \frac{2}{F_\pi^2}(L_9^r + L_{10}^r) + \frac{t_I^{CA}(0)}{12\pi m_\pi^2} \qquad (3)$$

Here, L_9^r and L_{10}^r are coefficients in the most general $O(E^4)$ chiral Lagrangian, renormalized at scale μ. The combination presented in d_0, d_2 is invariant under a change in μ. Eqn. (3) is valid up to higher order chiral correction of

order m_π^2. The Omnès function for $I = 0$ was obtained by Gasser et al. [18] from a detailed fit to the experimental data on $\pi\pi$ scattering, also incorporating the correct chiral behavior for the $\pi\pi$ amplitudes at low energy. The $I = 2$ Omnès function is not very important in the calculations and was obtained by a simple Padé approximation fit to the low energy $\pi\pi$ data. The remaining important ingredient, $t_I(s)$, is required by Low's theorem to approach the Born amplitude at low energy. At higher energies other intermediate states, due to ρ, ω exchange (i.e. $\gamma\pi \to \rho, \rho \to \gamma\pi$) are known to be present and are included with the coupling constant determined from $\rho, \omega \to \gamma\pi$ data. The combination of these ingredients is sufficient to accurately describe the data up to $s = 1\,GeV$ (see Fig. 1). For the region from 1 to $1.5\,GeV$ the dominant feature is the $f_2(1270)$ resonance in the $\pi\pi$ D-wave.

We wish to scale this result up in energy in order to describe $\gamma\gamma \to WW$ in one possible realization of a strongly interacting symmetry breaking sector. Specifically, our target theory is an $SU(N)$ gauge theory with a single doublet of fermions. Such a theory possesses an $SU(2)_L \times SU(2)_R$ global chiral symmetry, where dynamical symmetry breaking will also break the $SU(2)_L$ symmetry of the Standard Model. The pions of this gauge theory (called technipions below) are the Goldstone bosons which form the longitudinal components of the $W^\pm, Z^0$. This theory is the prototype of technicolor theories. As is well known, more ingredients must be added if one is to attempt to understand fermion masses. However, at present there is no simple way to extend the theory in order to obtain all desired results. The most essential ingredient for our calculations is the particle spectrum, specifically the techni-ρ, techni-ω and techni-f_2, and the absence of light states (L) which the technipions would scatter inelastically, $\pi_T\pi_T \to LL$. If extensions to the one doublet technicolor do not strongly modify these features, our calculation can remain valid.

The equivalence theorem states that the scattering amplitudes of longitudinal gauge bosons are related at high energy to those of the Goldstone bosons of the theory, in this case, to the technipions:

$$\mathcal{M}(\gamma\gamma \to W_L^i W_L^j) = \mathcal{M}(\gamma\gamma \to \pi_T^i \pi_T^j) + O(\frac{M_W}{\sqrt{s}}) \tag{4}$$

The restriction to high energies implies that any dependence on M_W must be small, and we will assume this to be true at $\sqrt{s} \geq 400\,GeV$. We will also

see that our ability to make predictions fail at about $\sqrt{s} = 3\,TeV$. Thus, we may expect that our calculations will be best applied between these two extremes.

In order to obtain the $\gamma\gamma \to WW$ amplitude we must i) scale energy variables up to the appropriate TeV scale and ii) modify the three ingredients described in regards the $\gamma\gamma \to \pi\pi$ calculations. The former is the simplest and best known. The vacuum expectation value $v = 246\,GeV$ plays the same role in the Standard Model as $F_\pi = 92.3\,MeV$ plays in QCD. However, in the large-N_c counting rules of QCD, $F_\pi = c\Lambda_{QCD}\sqrt{N_{TC}}$, where c is a dimensionless constant and Λ_{QCD} is the energy scale of QCD. Scaling this would require $v = c\Lambda_{TC}\sqrt{N_{TC}}$ with the same constant c and with Λ_{TC} being the energy scale of the $SU(N_{TC})$ theory. The scaling for all the normal resonances ($m_{X_T} \sim \Lambda_{TC}$) is then

$$m_{X_T} = m_X \frac{\Lambda_{TC}}{\Lambda_{QCD}} = m_X \frac{v}{F_\pi}\sqrt{\frac{N_c}{N_{TC}}} \tag{5}$$

This is the scaling for $X = \rho, \omega, f_2$.

The pion mass is of course an exception, since the quark masses of QCD have no counterpart in the technicolor theory. The technipion would be massless, but become the longitudinal component of the W. For kinematic reasons we will use $m_{\pi_T} = M_W$. However, the difference between $m_{\pi_T} = 0$ and $m_{\pi_T} = M_W$ is an $O(\frac{M_W}{\sqrt{E}})$ correction which is anyway below those predicted by the equivalence theorem.

In order to provide the remaining ingredients for the amplitudes (i.e. the substraction constant d_I, the Omnès function $D_I^{-1}(s)$ and the elementary amplitude $t_I(s)$), two sets of corrections must be made besides simply scaling the energy: i) Even for $N_{TC} = N_c = 3$, we must correct for the change in the technipion mass since

$$\frac{m_{\pi_T}}{\Lambda_{TC}} \ll \frac{m_\pi}{\Lambda_{QCD}} \tag{6}$$

and ii) in addition, if $N_{TC} \neq N_c$ we must correct for the changes in the scattering amplitude. The details and the results of each of the changes is given in Sect. III., while below we describe the general methods that we employ.

In some portions of the scattering amplitude it is easy to make the substitutions $(m_\pi, F_\pi) \Rightarrow (m_{\pi_T} = m_W, v)$. In particular we have analytic expressions for the Born and resonance exchange amplitudes and therefore these

present no problem in rescaling the Goldstone boson mass (we assume that the coupling constants for $\rho, \omega \to \pi\gamma$ have no significant dependence on the pion mass). However, the Omnès function is more difficult because it is based on physical data. As we explain in more detail in the next section, we get around this by using chiral symmetry to describe the pion mass dependence of the Omnès function at very low energy, and smoothly matching on the experimental data at high energy (where the mass dependence should be unimportant).

The substraction constants also depend on the pion mass, although in an indirect way. The renormalization prescription, adopted in Ref. [6], creates an implicit dependence in the renormalized chiral coefficients L_j^r on $\ln m_\pi^2$. This is easily corrected for via

$$L_j^r(m_2) = L_j^r(m_1) + \frac{\Gamma_j}{16\pi} \ln \frac{m_2}{m_1}. \tag{7}$$

The other set of corrections involve accounting for $N_{TC} \neq 3$. For this we use the large-N counting rules wherever possible. Most of these are obvious. The case that requires the most thought is the $I = 0$ Omnès function as it is determined by experimental data without a clear resonant behaviour. Our procedure here was to use chiral symmetry plus a Padé fit to the experimental Omnès functions in order to shift N_{TC}. The low energy chiral behavior is independent of N_{TC}, since v is held fixed but the first chiral correction is linear in N_{TC}. We note that our use of the Padé approximation only as a guide for estimating corrections to the experimental Omnès functions.

The above describes the main ingredients of our model. Basically we try to normalize our method to the succesful treatment of $\gamma\gamma \to \pi\pi$, and modify this by well-defined corrections. We implement this in the next section.

III. Details of the calculation

- *basics*

In this section we describe in detail how we calculate the $\gamma\gamma \to W^+W^-$ and $\gamma\gamma \to ZZ$ cross sections. We use the notation of Fig. 2 and we find that the gauge determined by

$$k_1 \cdot \epsilon_2 = k_2 \cdot \epsilon_1 = 0 \tag{8}$$

greatly simplifies our calculations. The scattering amplitude with totally polarized incoming photons [7], is required by Bose symmetry, Lorentz and gauge invariance to be equal to $\epsilon^1_\mu \epsilon^2_\nu \mathcal{M}^{\mu\nu}$ with

$$\begin{aligned}\mathcal{M}^{\mu\nu} &= 4ie^2\{A[k_2^\mu k_1^\nu - (k_1k_2)g^{\mu\nu}] + C\epsilon^{\mu\nu\alpha\beta}k_{1\alpha}k_{2\beta} \\ &\quad + B[\frac{(p_1k_1)(p_1k_2)}{(k_1k_2)} + p_1^\mu p_1^\nu - \frac{(p_1k_1)}{(k_1k_2)}k_2^\mu p_1^\nu - \frac{(p_1k_2)}{(k_1k_2)}k_1^\nu p_2^\mu]\} \qquad (9)\end{aligned}$$

In the neutral case an additional symmetrization in pion momenta is required. Parity invariance of EM and strong interactions requires $C = 0$ and the parity violation of the weak interactions is not important for the production of longitudinal gauge bosons. The polarization vectors of a totally polarized incoming photon are described in the helicity basis by two complex numbers as

$$\begin{aligned}\epsilon_1^\mu &= e_1^{(-)}\bar{\epsilon}^\mu + e_1^{(+)}\epsilon^\mu \\ \epsilon_2^\mu &= e_2^{(-)}\epsilon^\mu + e_2^{(+)}\bar{\epsilon}^\mu \qquad (10)\end{aligned}$$

Using this form and trivial kinematical considerations we arrive at

$$\begin{aligned}\mathcal{M} &= 2ie^2\{(As - m_\pi^2 B)[e_1^{(+)}e_2^{(+)} + e_1^{(-)}e_2^{(-)}] + \\ &\quad + Bp^2\sin^2\theta[e_1^{(+)}e_2^{(-)}e^{2i\phi} + e_1^{(-)}e_2^{(+)}e^{-2i\phi}]\} \qquad (11)\end{aligned}$$

where the helicity conserving amplitude, $As - m_\pi^2 B$, and the helicity flipping Bp^2 terms are clearly separated. It is now straightforward to calculate the cross sections [4]

$$\frac{d\sigma}{dt} = \frac{S\beta}{16(2\pi)^2 s}|\mathcal{M}|^2 \qquad (12)$$

where the statistical factor $S = 1$ for the charged pion final state and $S = 1/2$ for the neutral case. As dedicated $\gamma\gamma$ colliders mostly do not yield strongly polarized photons [19], we neglect photon polarization effects. Then, for completely unpolarized and uncorrelated incoming photons one has [4]

$$(\frac{d\sigma}{dt})_{unpol.} = \frac{2\pi S\alpha^2}{s^2}\{|As - m_\pi^2 B|^2 + \frac{|B|^2}{s^2}(m_\pi^2 - tu)^2\} \qquad (13)$$

As we have spin-1 incoming particles we must use the full lm partial wave expansion. The only existing waves are with $m = 2, 0, -2$ and we choose the normalization of the partial amplitude as

$$\begin{aligned}\mathcal{M} &= \sqrt{4\pi}2ie^2\sum_l\{Y_{l0}(\theta,\phi)[e_1^{(+)}e_2^{(+)}+e_1^{(-)}e_2^{(-)}]f^{l0}(s)+\\ &+Y_{l2}(\theta,\phi)[e_1^{(-)}e_2^{(+)}]f^{l2}(s)+Y_{l,-2}(\theta,\phi)[e_1^{(+)}e_2^{(-)}]f^{l,-2}(s)\}\end{aligned} \quad (14)$$

Inverting this formula we may connect the partial wave amplitudes to A and B:

$$\begin{aligned}f^{l0} &= \frac{\sqrt{2l+1}}{2}\int_{-1}^{1}dzP_l(z)(As-m_\pi^2B)\\ f^{l2}(s) &= \sqrt{\frac{2l+1}{(l-1)l(l+1)(l+2)}}\frac{1}{2}\int_{-1}^{1}dz\frac{1-z^2}{2}P_l^2(z)B\end{aligned} \quad (15)$$

Using isospin symmetry we may build the isospin-0 and isospin-2 amplitudes (there are no I=1 waves)

$$\begin{aligned}f_C^{lm}(s) &= \frac{2}{3}f_0^{lm}(s)+\frac{1}{3}f_2^{lm}(s)\\ f_N^{lm}(s) &= -\frac{2}{3}f_0^{lm}(s)+\frac{2}{3}f_2^{lm}(s)\end{aligned} \quad (16)$$

The idea of dealing with unknown technicolor models is to use their similarity to QCD pion production. There, according to the findings of [4], the main ingredients in the .5–1 GeV region (which will correspond to the TeV range in our case) are the Born+seagull amplitudes (only present in the charged channel), the vector and axial vector exchanges as dictated by a vector dominance model and final state pion rescattering which gives an important contribution to the neutral channel even near threshold. This model is known to reproduce the chiral results for low energy and assumes that rescattering is only important in the S-wave. For this reason we neglect all higher-wave rescattering and in the S-wave we also assume the validity of Watson theorem. In QCD this is true even above multipion thresholds and only breaks down at two-kaon threshold. As in our model we have no kaon we may suppose its validity all the way up to the f_2 mass range.

Then, in a way similar to [4], we add the Born and full vector-dominance amplitudes to S-wave rescattering. The latter is handled by writing a doubly subtracted dispersion relation for $f_I(s) \equiv f_I^{00}$ [4]

$$f_I(s) = p_I(s) + D_I^{-1}(s)\{(c_I + sd_I) - \frac{s^2}{\pi}\int_{4m_\pi^2}^{\infty} \frac{dx}{x^2}\frac{p_I(x) Im D_I(x)}{x - s - i\epsilon}\} \qquad (17)$$

where $p_I(s)$ is the partial amplitude from Born + vector dominance contributions; the Omnès functions

$$D_I(s) = exp\{-\frac{s}{\pi}\int_{4m_\pi^2}^{\infty} \frac{ds^{'}}{s^{'}}\frac{\delta_I(s)}{s^{'} - s - i\epsilon}\} \qquad (18)$$

establish a connection to the $\pi\pi$ elastic phase shifts. The question of subtraction constants is reviewed in [4] and we simply quote the results, $c_I \equiv 0$ (to satisfy Low's theorem) and

$$d_I = \frac{t_I^{CA}(0)}{12m_\pi^2} \qquad (19)$$

to satisfy the chiral constraint (t_I^{CA} are the Weinberg scattering amplitudes so d_I doesn't really depend on m_π). Note that since vector and axial vector mesons generate $L_9 + L_{10}$, the effect of the chiral coefficients $L_9 + L_{10}$ also appears in $p_I(s)$ rather than in d_I, in contrast to the form in Eqn. 2.

The particular form of the vector dominance model we use is also taken from [4], together with the QCD vector meson–pion–photon coupling constants $R_\omega = 1.35\, GeV^{-2}$ and $R_\rho = 0.12\, GeV^{-2}$. It includes the ω and ρ mesons in narrow-width approximation and also $a_1(1270)$ which is found to have a large contribution to $\gamma\gamma \to \pi^0\pi^0$. Their contribution into A and B are worked out in full detail in [4], Eqns. (35),(37):

$$\begin{aligned} sA^0 &= -\frac{s}{2}\sum_{V=\rho,\omega} R_V(\frac{m_\pi^2 + t}{t - m_V^2} + \frac{m_\pi^2 + u}{u - m_V^2}) \\ B^0 &= -\frac{s}{2}\sum_{V=\rho,\omega} R_V(\frac{1}{t - m_V^2} + \frac{1}{u - m_V^2}) \end{aligned} \qquad (20)$$

and

$$sA^+ = -\frac{s}{2}R_\rho(\frac{m_\pi^2 + t}{t - m_\rho^2} + \frac{m_\pi^2 + u}{u - m_\rho^2}) + m_A^2 s\frac{L_9^r + L_{10}^r}{F_\pi^2}(\frac{1 - \frac{m_\pi^2 + t}{2m_A^2}}{t - m_A^2} + \frac{1 - \frac{m_\pi^2 + u}{2m_A^2}}{u - m_A^2})$$

$$B^+ \;=\; -(\frac{1}{t-m_\pi^2}+\frac{1}{u-m_\pi^2})-\frac{sR_\omega}{2}(\frac{1}{t-m_\rho^2}+\frac{1}{u-m_\rho^2}) \tag{21}$$

We cut off the cross section is at $Z \equiv cos\Theta = 0.6$. This, in addition to trying to mimic the experimental limitation, serves another purpose: most of the W^+W^- events go into forward direction and constitute a huge background which is greatly reduced this way [15]. The cross section is given by

$$\int_{t_a}^{t_b} dt \frac{d\sigma}{dt} \quad \text{with} \quad t_{b,a} = m_\pi^2 - \frac{s}{2}(1 \mp \beta Z) \tag{22}$$

This integration can be made by hand, and we calculated the dispersive integral numerically.

- *1/N: meson masses and couplings*

As we mentioned in Sect. II., QCD results have to be generalized to different numbers of colors, and we take the required additional information from the leading $1/N_{TC}$ behaviour. In the following we find the leading $1/N_{TC}$ behaviour of the couplings of vector and axial vector mesons, namely R_ρ, R_ω and $L_9 + L_{10}$. They are restricted by the Weinberg sum rules [8], which in the narrow width approximation read

$$F_\pi^2 = F_\rho^2 - F_{a_1}^2 \quad and \quad F_\rho^2 m_\rho^2 = F_{a_1}^2 m_{a_1}^2 \tag{23}$$

These restrictions imply that F_V and F_A are constants in $1/N_{TC}$. Their connection to the constants of equations (20) and (21) can be seen simply on dimensional grounds,

$$R_V = c\frac{F_V^2}{m_V^4} \tag{24}$$

with c being a dimensionless constant for vectors and F_A can be taken from [8]

$$L_9 + L_{10} = \frac{F_A^2}{m_A^2} \tag{25}$$

All this means that the needed $1/N_{TC}$ rules are

$$L_9 + L_{10} \sim N_{TC} \quad and \quad R_V \sim \frac{N_{TC}}{m_\rho^2} \tag{26}$$

- *pion scattering amplitudes*

There is an important and interesting physics in the outgoing pion rescattering process. To describe it, we need to know the Omnès functions from somewhere. These are connected to the $\pi\pi$ elastic phase shifts as long as the elastic process dominates. Our description is consequently limited to this energy region; fortunately this means $\sim 1\,GeV$ in QCD. In terms of technicolor this scales up to $2.6\,TeV$ for $N_{TC} = 3$, even for $N_{TC} = 10$ we still may expect a relatively good description at $1.4\,TeV$. The fact that in our model there are no kaons may push that limit even a little further. Nevertheless, we do not expect to have the right description above the (techni)f_2 resonance and we simply neglected the tail of the dispersion integral which comes from energies above $3\,TeV$. Several reruns with different energy cutoffs showed little effect.

For the $N_{TC} = 3$ case a simple rescaling of the known Omnès functions is possible. However, if we want to generalize our statements for higher N_{TC}'s – there is no reason to expect that technicolor is just a copy of QCD – we need a deeper understanding of the phase shifts. For the region $s < 0.1\,GeV^{-2}$ (as in QCD) chiral perturbation theory gives a satisfactory description, but a second order (in s) calculation shows that some uniterization is necessary. We did this, using [1,1] Padé approximation [4]

$$\begin{aligned} ReD_I^{Padé}(s) &= 1 - sc_I + t_I^{CA}(s)\frac{2}{\pi}[\frac{\beta}{2}\ln\frac{s(1+\beta)^2}{4m_\pi^2} - 1] \\ ImD_I^{Padé}(s) &= -\beta t_I^{CA}(s) \end{aligned} \tag{27}$$

Although we know that this procedure only gives an approximate result, we use it as a vehicle for introducing modifications to the experimental Omnès functions. In (27), the constants c_I are expressed by a certain linear combinations of chiral coefficients

$$c_I = \frac{l_I^r(m_\pi)}{f_\pi^2} \tag{28}$$

and they pick up logarithms in the chiral limit.

In the standard chiral renormalization scheme, the chiral coefficients l_I contain factors of $\ln m_\pi^2$. For our purposes it is better to remove these so that we define $\bar{c}_I = \frac{\bar{l}_I^r}{f_\pi^2}$, with

$$\begin{aligned} ReD_I^{Padé}(s) &= 1 - s\bar{c}_I(\mu) + t_I^{CA}(s)\frac{2}{\pi}[\frac{\beta}{2}\ln\frac{s(1+\beta)^2}{4\mu^2} - 1] + \\ & [\frac{\beta}{\pi}t_I^{CA}(s) - \frac{\gamma_I}{32\pi^2 f_\pi^2}s]\ln\frac{\mu^2}{m_\pi^2} \end{aligned} \tag{29}$$

where the numbers γ_I govern the chiral logarithms

$$\bar{l}_I^r = l_I^r + \frac{\gamma_I}{32\pi^2}\ln\frac{\mu^2}{m_\pi^2} \tag{30}$$

As the Omnès functions are known to have a finite chiral limit (i.e. $\delta_I(s) = s \times (\textit{finite})$) we conclude that the quantity in the square brackets vanishes in that limit, yielding $\gamma_0 = 2$ and $\gamma_2 = -1$.

The chiral amplitude also depends directly on N_{TC}. To determine this dependence we use the succesful model of the chiral constants, expressed in terms of resonance saturation. This again comes from matching chiral symmetry with vector dominance [16]

$$l_I^r(m_\rho) = (const)\frac{\Gamma_\rho F_\pi^4}{m_\rho^5} = O(N_c) \tag{31}$$

This form requires that the leading $1/N_{TC}$ behaviour to be

$$\bar{c}_I^{TC}(\mu) = \frac{N_{TC}}{3}\{\frac{f_\pi^2}{F_\pi^2}\bar{c}_I^{QCD}(\mu^{QCD}) + \frac{\gamma_I}{16\pi^2 F_\pi^2}\ln(\frac{\mu^{QCD}}{m_\rho^{QCD}}\frac{m_\rho^{TC}}{\mu})\} \tag{32}$$

As an input we still need a value for $\bar{c}_I^{QCD}(\mu^{QCD} = 140\,MeV)$. Plotting several values on Fig. 9, using the method of trial and error, we have the best fit when $\bar{c}_0^{QCD}(\mu^{QCD} = 140\,MeV) = 1.5 \pm 0.2$ and $\bar{c}_2^{QCD}(\mu^{QCD} = 140\,MeV) = -1.7 \pm 0.5$.

- *Inclusion of f_2*

In $\gamma\gamma \to \pi\pi$ scattering an important feature in the direct channel is the f_2 resonance, so we may reasonably suspect that incorporating a corresponding technimeson may be important. This is especially true for larger N_{TC}'s where meson resonances come down in mass and become narrower.

As f_2 is a tensor particle its couplings require special consideration. It is not present in the crossed channels as C-invariance forbids $f_2 \to \gamma\pi$, and, as we saw that $\mathcal{F}(\gamma\gamma \to \pi\pi)$ is generally described in terms of two amplitudes, the description of f_2 requires information on two coupling constants, in terms of the two possible photon helicity differences. When we turn to the existing experimental data on $\gamma\gamma \to \pi\pi$ [14], we see that there is a controversy in determining the ratio of different waves near f_2 mass. It had been generally accepted that the interaction is pure $|JJ_3>= |22>$, and although [14] argues that the presence of a $|20>$ interaction is favored, but its significance is rather poor ($\chi^2/N_{DF} \sim 1.8 - 2.0$ for $N_{DF} = 177$) and as long as data with scattering angle cut $|Z| < 0.6$ are concerned, they may be explained by the conservative hypothesis of $|22>$ dominance. This assumption means, in terms of the amplitudes of (13), that we have no impact of f_2 in $(As - m_\pi^2 B)$ and the *same* t-independent quantity $\mathcal{F}_{22}(s)$ is added to B_C and B_N. For simplicity we suppose that this amplitude is of a pure Breit-Wigner form

$$\mathcal{F}_{22}(s) = \frac{\mathcal{F}_{22}}{s - (m_{f_2}^2 - \frac{i}{2}\Gamma_{f_2})^2} \tag{33}$$

.

In the case of a single-channel resonance $\mathcal{F}_{22}$ is required to be real. Its value is determined by the well-known Breit-Wigner formula

$$\sigma_{\pi^+\pi^-}^{unpol} = \frac{40\pi}{s} \frac{\Gamma_{f_2\to\pi\pi}\Gamma_{f_2\to\gamma\gamma} m_{f_2}}{|s - m_{f_2}^2 + i m_{f_2}\Gamma_{f_2}|^2} \tag{34}$$

and this is to be compared to the *pure* Breit-Wigner form of the amplitude

$$\sigma_{\pi^+\pi^-}^{unpol} = \frac{2\pi\alpha^2}{s^2} \frac{|\mathcal{F}_{22}|^2}{|s - m_{f_2}^2 + i m_{f_2}\Gamma_{f_2}|^2} \int_{t_a}^{t_b} dt \frac{(m_\pi^4 - tu)^2}{s^2} \tag{35}$$

This implies

$$|\mathcal{F}_{22}| = \frac{20}{\alpha m_{f_2}} \sqrt{\Gamma_{f_2\to\pi\pi}\Gamma_{f_2\to\gamma\gamma}} \tag{36}$$

and the sign of $\mathcal{F}_{22}$ is found by fitting the results to the experimental data. To this end, we plotted on Fig. 3 and Fig. 4 the full $\gamma\gamma \to \pi\pi$ cross sections with both negative and positive $\mathcal{F}_{22}$. Although the neutral pion channel is inconclusive, comparing Fig. 3 to the corresponding experimental values (that is, to Fig. 4a in [14]), we clearly see that $\mathcal{F}_{22}$ must be negative as the vector meson contribution and the resonance have a clear destructive interference just above, while a positive interference below resonance. The dispersive integral gives very little contribution in this range. The correctness of the shape of our curve and its numerical height supports our assumption that we may neglect $|10>$ contributions to the s-channel f_2 contribution.

We take the numerical values as given by the Particle Data Group [17]

$$\Gamma_{f_2\to\gamma\gamma} = 2.6\, keV \ , \ \Gamma_{f_2\to\pi\pi} = 0.84\Gamma_{f_2} \ , \ \Gamma_{f_2} = 185\, MeV \tag{37}$$

These considerations allow us to calculate the impact of a QCD-like techni-f_2 on $W_L^+W_L^-, ZZ$ production. We still have to see how $\mathcal{F}_{22}$ changes with N_{TC}. As we have no chiral prediction at this high energy we go back to conventional $1/N$ arguments. Then, as seen from Fig. 5,

$$\Gamma_{f_2\to\gamma\gamma}/\Gamma_{f_2\to\pi\pi} = O(e^4N^2) \tag{38}$$

which yields, in terms of the coupling constant

$$|\mathcal{F}_{22}^{TC}| = \frac{20}{\alpha}\sqrt{\frac{\Gamma_{\gamma\gamma}^{TC}\Gamma_{\pi\pi}^{TC}}{(m_{f_2}^{TC})^2}} = \frac{20}{\alpha}\sqrt{\frac{\Gamma_{\gamma\gamma}^{TC}\Gamma_{\pi\pi}^{TC}}{(m_{f_2}^{QCD})^2}} = |\mathcal{F}_{22}^{QCD}| \tag{39}$$

This enhancement of the $\gamma\gamma$ branching ratio makes the techni-f_2 resonance *the* important feature of ZZ production at higher N_{TC}.

- *Vector meson form factors*

The vector meson dominance amplitude as given by (20,21) has an incorrect high energy behaviour. For example, a simple counting of factors of s shows that σ_N grows as $O(s)$ and this obviously violates unitarity. To cure this, we realize that all vector mesons are extended objects of about the same size, and their interactions should be described by form factors. The same

power counting shows that a factor of $(m_\pi^2 + t)$ in the vector propagator numerators is responsible for the leading high energy behaviour, and this goes back to the momentum-squared terms describing longitudinal vector meson contributions. Fig. 8 shows what we get using 'pointlike' vector mesons (e.g. constant form factors). The high energy increase obviously contradicts to the experimental data.

For each of the vertices in Fig. 6 we have a separate form factor. There action is described by taking the vector meson coupling constants R_ω, R_ρ and R_A as functions of t in the form

$$G = \frac{G(t=0)}{1 - t/M^2} \tag{40}$$

As we will see these form factors have little effect below $s = m_{f_2}$, this simple form is acceptable with $M \sim m_\rho$. The integrations, similar to the ones in (20), yield formulas which, in some energy ranges, represent the difference of large and almost cancelling quantities, so their evaluation has been done by 16-byte arithmetics. Indeed, as curves on Fig. 7 shows, only cross section near and above m_{f_2} are affected.

IV. Discussion

A high luminosity $\gamma\gamma$ collider is not yet feasible at the energies required for gauge boson production. However the concept is attracting attention and it is possible that it may in the future become a reality. If a Higgs boson is not found at lower energies, the study of $\gamma\gamma \to W^+W^-, Z^0Z^0$ will be one of the physics goals of such a facility. The present calculation is the best description that we are able to provide for these reactions in a particular type of theory, closely related to QCD. Most of the features of the QCD reaction $\gamma\gamma \to \pi\pi$ are visible in our result, although they are somewhat modified by changes in the Goldstone boson mass and the possibly different gauge group.

The main results of our calculations are shown on Fig. 10 a,b. Comparing them to the analysis of experimental possibilities in Ref. [3], we conclude that, with the presently envisaged parameters of a $\gamma\gamma$ collider, which may be realized on a linear TeV electron accelerator with laser beam backward scattering [19], the $\gamma\gamma \to W_L^+W_L^-$ process is clearly visible in two regions.

i) below $\sim 500\ GeV$, where the validity of our calculations is restricted by the applicability limit of the equivalence theorem, and ii) on the f_2 resonance. This is a huge resonance and its existence would be a clear signal for a technicolor-like model, yielding in the same time information on the value of N_{TC}. In the case of the $\gamma\gamma \to Z_L Z_L$ reaction, a similar statement says that the only really observable feature is the f_2 resonance, at presently proposed luminosities.

It would also be interesting to contrast these results with a different strongly interacting symmetry breaking mechanism, that of a very heavy Higgs boson. However, the latter theory may even be difficult to define, as the studies of triviality of the Φ^4 theory mean that a very heavy Higgs is not possible unless other new physics enters the theory.

Appendix: loop diagrams and the equivalence theorem

The equivalence theorem [20][21][22][23] says that the interactions of *external* longitudinal gauge bosons and the corresponding Goldstone bosons are equal at high energy. However, to our knowledge, the proofs do not address the issue of whether there is also an equivalence for particles inside loop diagrams. For example, in chiral perturbation theory, loop diagrams involve the Goldstone bosons. Do they accurately reflect the effect of W_L loops? We do not have a general answer here. However, for our process we are able to assure ourselves that such use is allowed. This is because we are able to reformulate the problem as a dispersion relation, which only involves external Goldstone bosons. The ingredients to the dispersion relation are the $\gamma W_L \to \gamma W_L$ and the $W_L^+ W_L^- \to W_L^+ W_L^-$ scattering amplitudes and the substraction constants. All can be defined for external particles. However in [4] it was shown how the choice of the lowest order chiral amplitudes for these quantities exactly reproduces the result of the set of Feynmann diagrams in chiral perturbation theory.

The only possible remaining problem could be the sensitivity to the low momentum region inside the loop integrals, where there is no equivalence between W_L and the Goldstone bosons. If the loops were infrared dominated, the infrared contribution would not be trustworthy. Fortunately chiral amplitudes vanish at zero momentum, so that the infrared region is not too important. This also can seen by the fact that the factor of $\ln m_\pi^2$ vanish and the result has a smooth limit as $m_\pi \to 0$. We have also checked that truncating the dispersion integrals at low energies has little effect on the resulting cross sections.

References

[1] A recent review is Chanowitz M., in "Perspectives on Higgs Physics", ed. Kane G. (World Scientific, 1993). See also Bagger J., Dawson S., Valencia G., Phys. Rev. Lett. **67**, 2256 (1991).

[2] Dicus D., Kas C., Texas Preprint CPP-93-24, Abbasabadi A. et al., MSUTH-92-03.

[3] Herrero M.J., Ruiz-Morales E., Phys. Lett. **B296**, 397 (1992).

[4] Donoghue J.F., Holstein B.R., Phys. Rev. **D48**, 137 (1993).

[5] Gasser J., Bellucci S., Sainio M., to be published.

[6] Gasser J. and Leutwyler H., Nucl. Phys. **B250**, 465 (1985).

[7] Ko P., Phys. Rev. **D41**, 1531 (1990).

[8] Donoghue J.F., Holstein B.R., Wyler D., Phys. Rev. **D47**, 2089 (1993).

[9] Morgan D, Pennington H.R., Phys. Lett. **B272**, 134 (1990).

[10] Peccei R.D., Solà J., Nucl. Phys. **B281**, 1 (1987).

[11] Donoghue J.F., Ramirez C., Valencia G., Phys. Rev. **D38**, 2195 (1988).

[12] Leutwyler H., Gasser J., Ann. Phys. **158**, 142 (1984).

[13] Riggenbach C et al., Phys. Rev. **D43**, 127 (1991).

[14] Morgan D., Pennington H.R., Zeitschrift für Physik **C48**, 623 (1990).

[15] Chanowitz M.S., LBL-31697 (1992).

[16] Donoghue J.F., Ramirez C., Valencia G., Phys. Rev. **D39**, 1947 (1989).

[17] Review of Particle Properties, Phys. Lett. **B239**, p.VII.27 (1990).

[18] J.Gasser, as given in Donoghue J.F., Gasser J. and Leutwyler H., Nucl. Phys. **B343**, 341 (1990).

[19] Telnov V.I., Nucl. Instr. and Methods in Phys. Res. **A294**, 72 (1990).

[20] Cornwall J.M., Levin D.N., Tiktopoulos G., Phys. Rev. **D10**, 1145 (1974).

[21] Chanowitz M.S., Gaillard M.K., Nucl. Phys. **B261**, 379 (1985).

[22] Lee B.W., Quigg C, Thacker H.B., Phys. Rev. **D16**, 1519 (1977).

[23] Bagger J., Schmidt C., Phys. Rev. **D41**, 264 (1989).

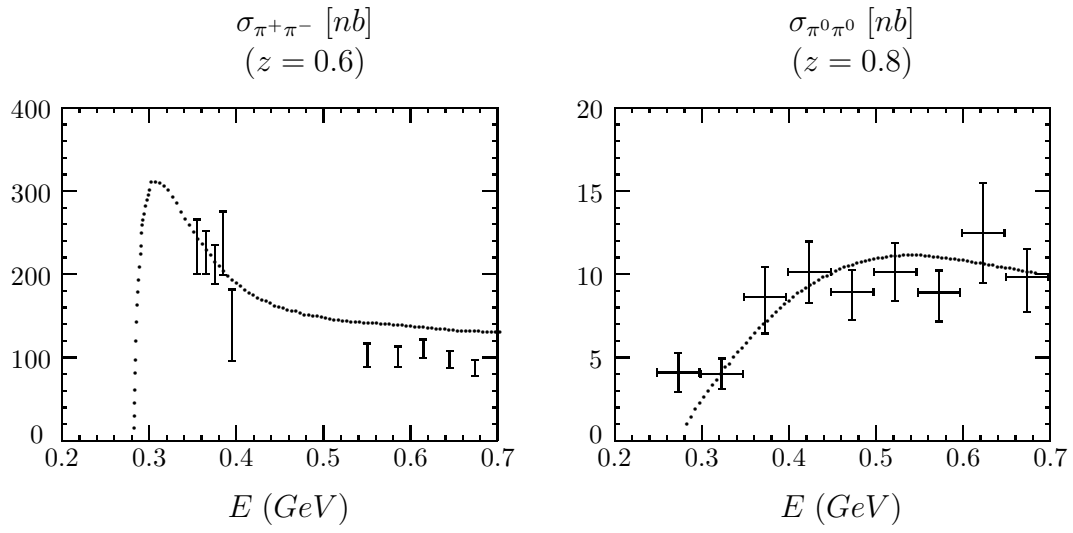

Figure 1. Total $\gamma\gamma \to \pi^+\pi^-$ and $\gamma\gamma \to \pi^0\pi^0$ cross sections with a forward cut at $|\,z\,| \equiv |\cos\Theta|$, figures taken from [4].

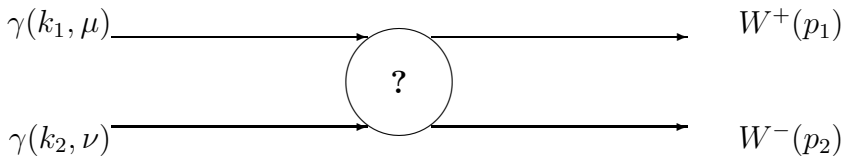

Figure 2. Explanation of the kinematic conventions used in the text.

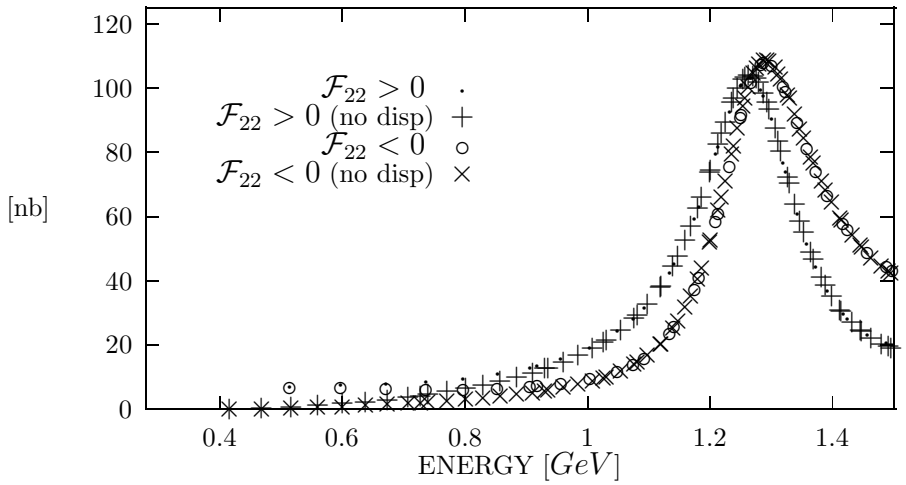

Figure 3. $\gamma\gamma \to \pi^0\pi^0$ cross section with forward cut at $\mid Z \mid \equiv \mid \cos\Theta \mid < .6$.

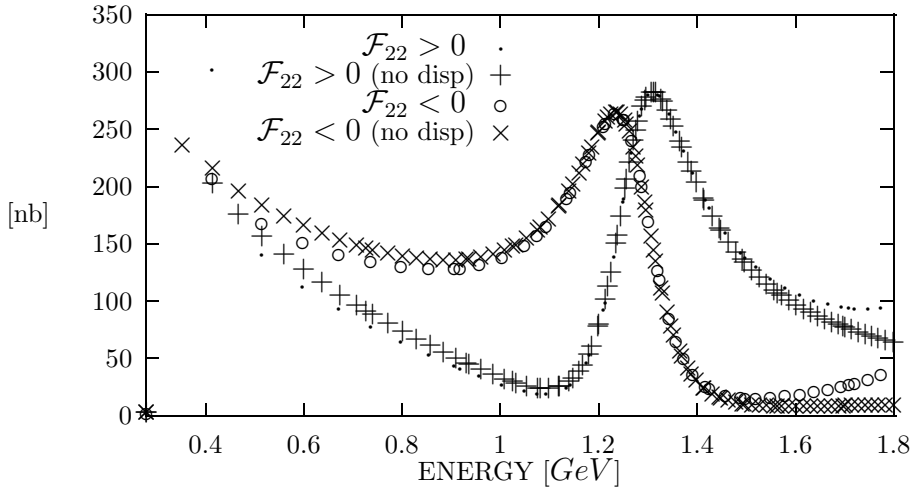

Figure 4. $\gamma\gamma \to \pi^+\pi^-$ cross section with forward cut at $\mid Z \mid \equiv \mid \cos\Theta \mid < .6$. Note that at f_2 resonance the dispersion integral is unimportant ('no disp' means that the dispersion integral and the substraction terms are left out).

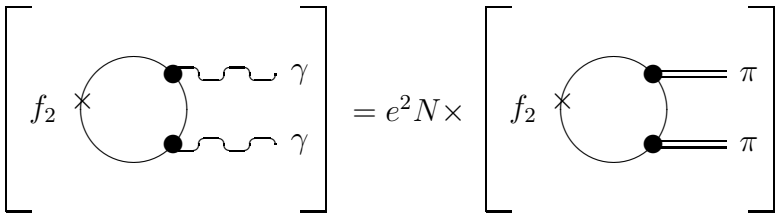

Figure 5. $1/N$ power counting diagrams for f_2 interactions.

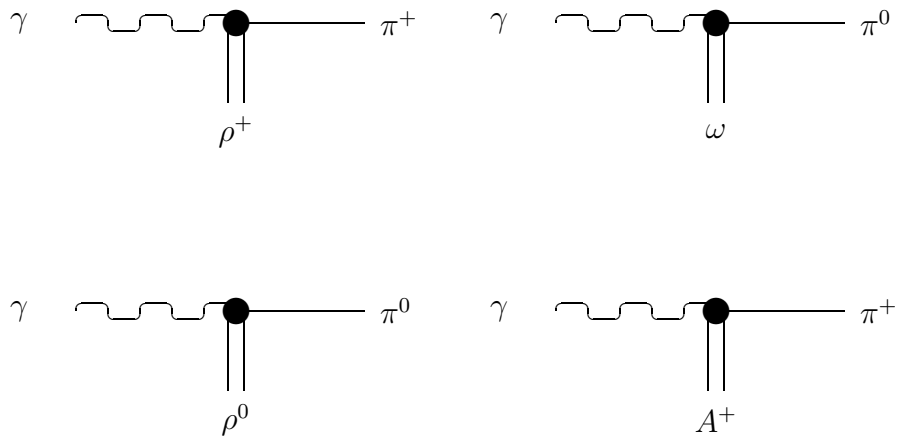

Figure 6. Vector meson – photon – pion vertices: these pick up form factors at $t \geq m_\rho^2$.

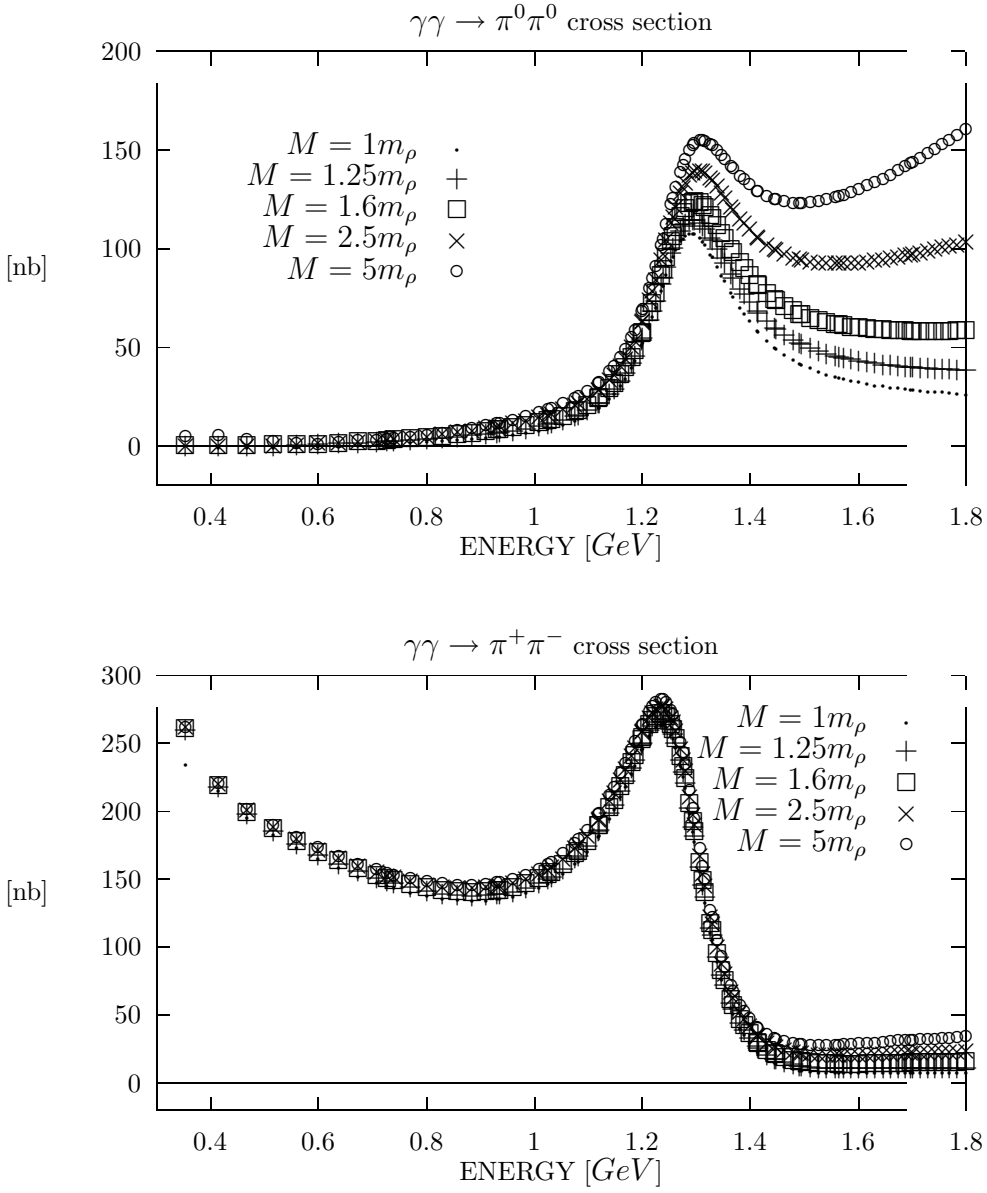

Figure 7 a,b. The impact of the form factors on $\gamma\gamma \to \pi\pi$ cross sections.

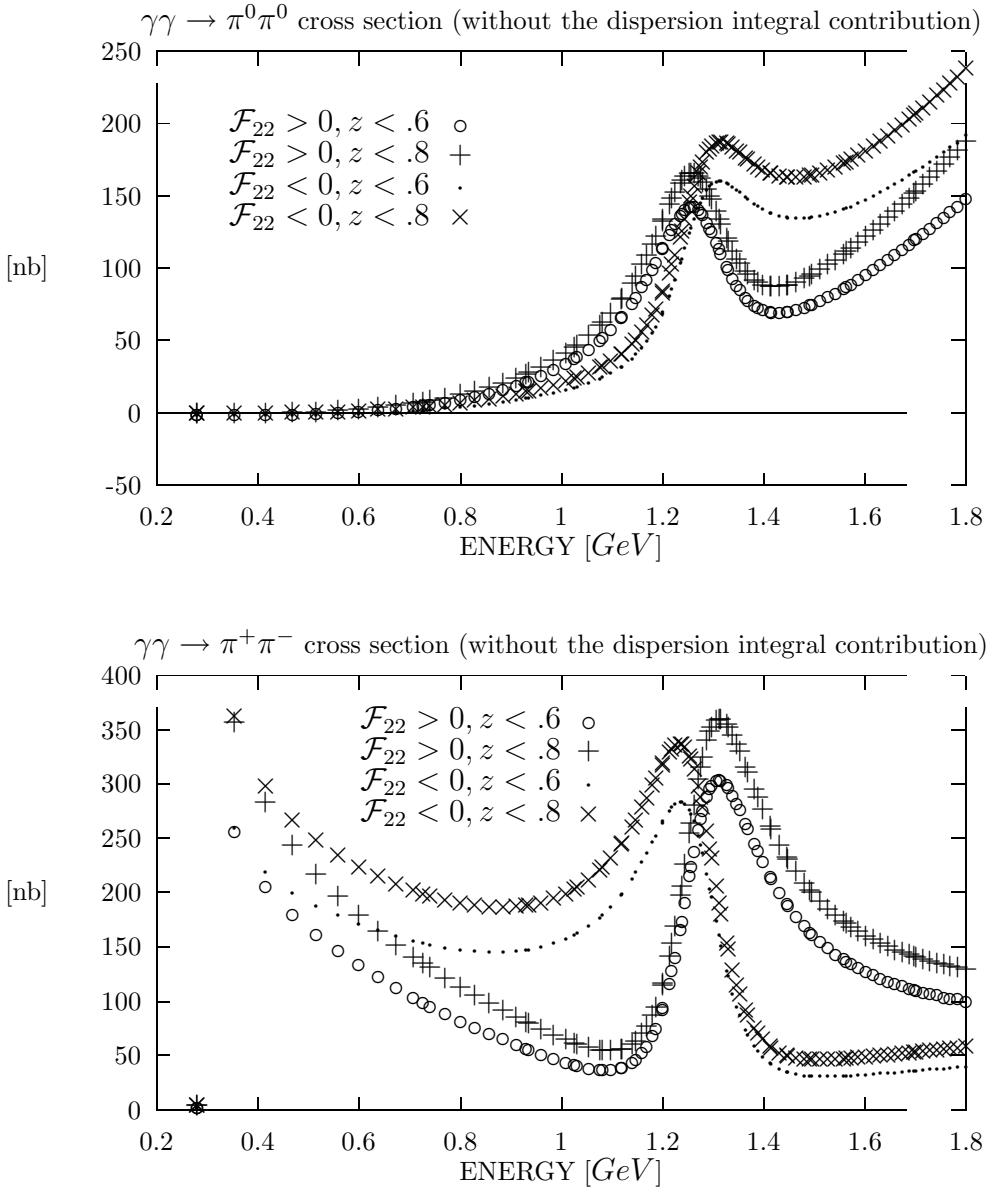

Figure 8 a,b. Pointlike vector mesons would generate an increase in $\gamma\gamma \to \pi\pi$ cross sections and would even make it hard to determine the sign of $\mathcal{F}_{22}$.

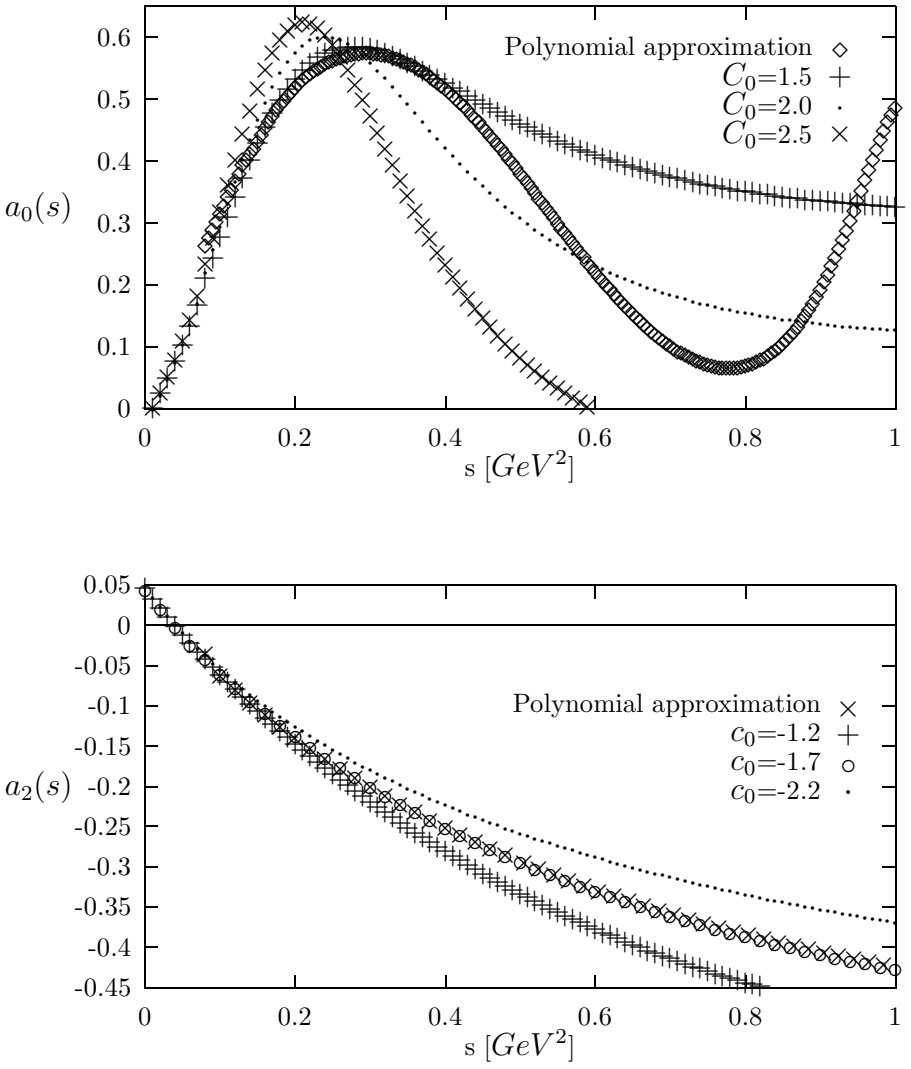

Figure 9 a,b. Padé approximation to the real part of the isospin-0 and isospin-2 $\pi\pi$ elastic scattering amplitude. The curves signed 'polynomial approximation' are a) for $I = 0$ fitted Gasser's data [18], corrected to have correct chiral behaviour at low s, b) fitted similarly to Padé approximants of [4] and to the linear chiral prediction.

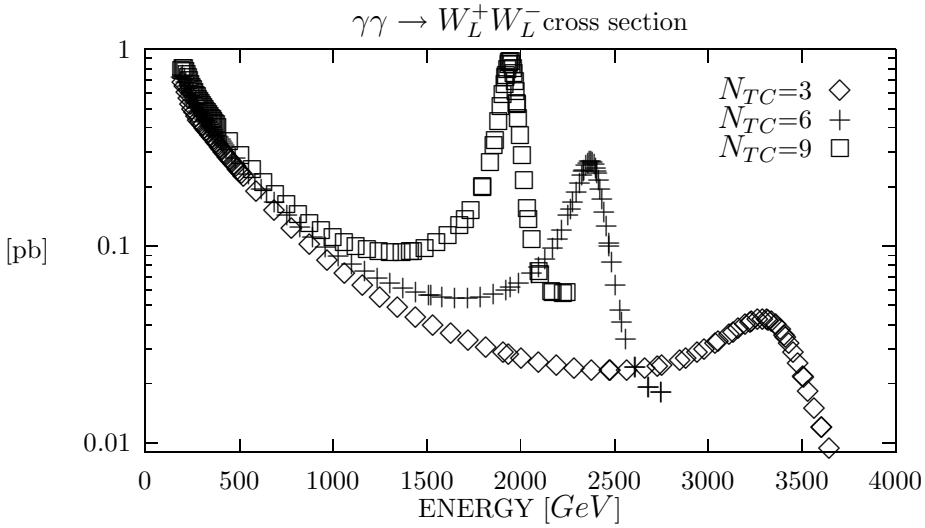

Figure 10 a. The total $\gamma\gamma \rightarrow W_L^+W_L^-$ cross section as a function of $\sqrt{s}$ and N_{TC}. Note the strong dependence of the f_2 peak on technicolor number.

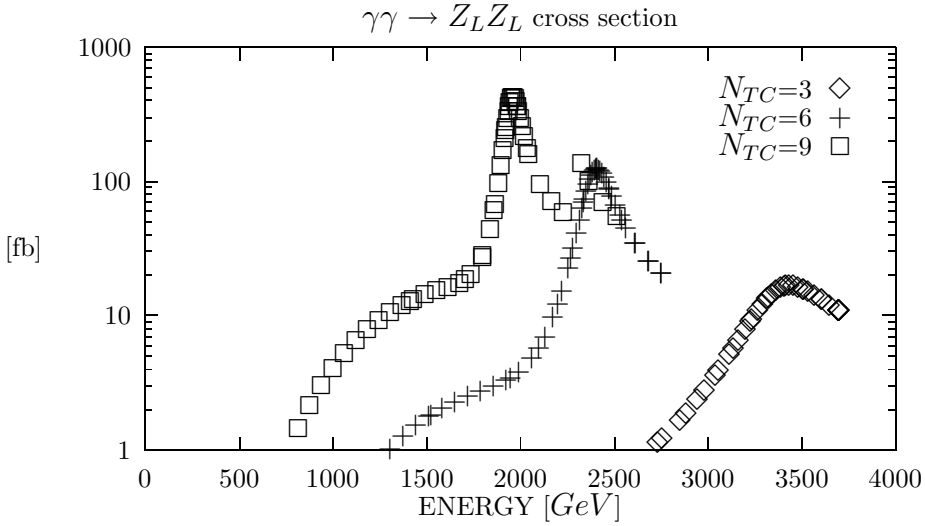

[6 [6

Figure 10 b. The total $\gamma\gamma \rightarrow Z_LZ_L$ cross section as a function of $\sqrt{s}$ and N_{TC}. Rescattering and vector meson dominance effects are similar in magnitude for $\sqrt{s} < (1\,TeV)^2$ but both are small.